Supplementary Material for "Vacuum ultraviolet photoionization cross section of the hydroxyl radical"

Leah G. Dodson[1], John D. Savee[2], Samer Gozem[3], Linhan Shen[1], Anna I. Krylov[3], Craig A. Taatjes[2], David L. Osborn[2], Mitchio Okumura[1]

[1]*Division of Chemistry and Chemical Engineering, California Institute of Technology, Pasadena, California, 91125, USA*

[2]*Combustion Research Facility, Sandia National Laboratories, Livermore, California, 94551, USA*

[3]*Department of Chemistry, University of Southern California, Los Angeles, California, 90089, USA*

I. DETERMINING THE OZONE CONCENTRATION

The ozone concentration in the cell was based on measurements of the ozone mixing ratio after the ozonizer, prior to dilution, using an ozone monitor (uncertainty 2%). As mentioned in the text, the ozone mixing ratio delivered to the monitor exceeded the rated range by as much as a factor of 5. To test the accuracy of the estimated ozone concentrations, we compared the absolute photoionization cross section of ozone derived from the measured ion signal to literature values of the photoionization cross section.

Berkowitz recently evaluated the literature value for the absolute ozone photoionization spectrum.[1] There were three previous measurements of ozone photoionization. Cook reported a total photoabsorption cross section at a single photon energy.[2,3] More recently, there were two relative partial cross section measurements. Mocellin *et al*.[4] (energy resolution 20–40 meV) and Weiss *et al*.[5] (5–10 meV resolution) detected O_3^+ photoions and both fragment ions O_2^+ and O^+. Berkowitz scaled these two spectra to the Cook cross section to obtain the absolute partial-photoionization spectra shown in Figure S1. Berkowitz does not provide an error estimate for these spectra.

We obtained the absolute ozone partial-photoionization spectrum from the O_3^+ signal using the ozone concentration in the cell derived from the ozone monitor measurements. This cross section was determined relative to that of O(^3P).[6] The absolute ozone photoionization spectrum (shown in Fig. S1, black open circles) agrees well, both in terms of shape and absolute magnitude (to within 25%), with the Weiss/Berkowitz spectrum.

Since the m/z = 48 ozone ion signal was linear with the expected ozone concentration in the cell, we concluded that the ozone monitor, although operating outside its specified range, gave accurate ozone concentrations. The uncertainty in ozone concentration (4.5%) was from the error in calculating the dilution, with the 4% of full scale error in the O_3/O_2 flow specified for the variable rotameter and the 2% uncertainty in the ozone monitor reading.

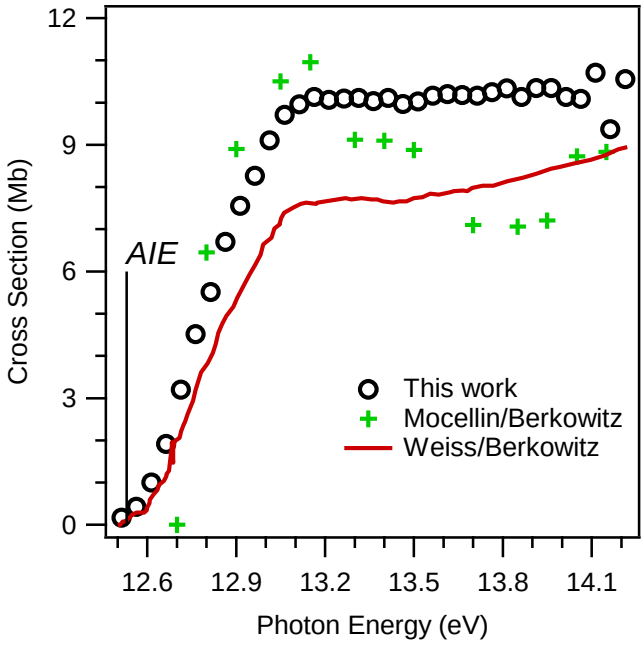

FIG. S1. Absolute photoionization spectrum of ozone. Shown here (black circles) is the absolute photoionization spectrum of ozone measured in this work, which assumes that the reading of the ozone monitor is accurate. Also shown here are the literature absolute photoionization spectra of ozone of Mocellin[4] (green pluses) and Weiss[5] (red line), as evaluated by Berkowitz.[1]

II. LITERATURE PHOTOIONIZATION SPECTRUM OF O(^3P)

In the main text, we used the O(^3P) absolute photoionization spectrum to calibrate the OH spectrum at 14.193 eV. For this purpose, we digitized the relative spectrum shown by Dehmer *et al.*[7] and scaled the spectrum at 14.25 eV—a region that is flat and free of resonances—to the absolute photoionization cross section (3.1 Mb) reported by Angel and Samson at the same energy.[6] Although Fennelly and Torr[8] provide a tabulated spectrum using the same procedure, inconsistencies appear between the tabulated data and the original spectrum. We will discuss these differences in this section.

In 1992 Fennelly and Torr evaluated the photoionization and photoabsorption cross section of O(^3P) from 1027.0 to 23.7 Å (12.0–523 eV).[8] In their evaluation, they used absolute photoionization cross section measurements, made by Angel and Samson[6] and Samson and Pareek,[9] to place the high-resolution relative O(^3P) spectrum measured by Dehmer *et al.*[7] on an absolute scale. The relative spectrum was scaled to the cross section measurements made in the part of the spectrum that is relatively flat: between 13.6–16.2 eV. The tabulated data, presented by Fennelly and Torr, was taken from Table I of their paper and is plotted in Figure S2 (black dots). In the plotted spectral region (between 13.5 and 14.5 eV), the point with maximum intensity at the resonance was given at 14.11 eV with an intensity of 34.88 Mb, as shown. This is contradictory to the spectrum presented by Fennelly and Torr (Figure 2 of their paper), which indicates that the intensity of this resonance is 210.4 Mb.

We digitized the spectrum presented by Dehmer *et al*. (Figure 2 in their paper)[7], using the digitization program in OriginPro, and normalized that relative spectrum to the absolute value reported by Angel and Samson[6] at 14.25 eV (3.1 Mb). The resulting spectrum is shown in Figure S2 (red line). The maximum intensity of the digitized spectrum occurs at 14.12 eV with an intensity

of 211 Mb, in good agreement with the plotted spectrum presented by Fennelly and Torr. Additionally, the flat regions of the spectrum agree well with the cross section values reported by Fennelly and Torr. However, the Fennelly and Torr spectrum (from both Table I and Figure 2 of Fennelly and Torr's paper) shows significant broadening to the resonance that does not appear in the original spectra presented by Dehmer *et al*.

Because of the discrepancies, we feel that, by going back to the original Dehmer *et al*. data (which is nearly the same resolution as this work), we can correctly use the digitized spectrum in comparing these works (shown in the manuscript in Figure 5). Although much of the O(^3P) spectrum is flat, it was necessary to reevaluate the literature O(^3P) spectrum because our experiments at 14.193 eV would have been affected by the erroneous broadening of the resonance centered at 14.12 eV. We advise authors to use care in using the literature spectrum in the region near resonances.

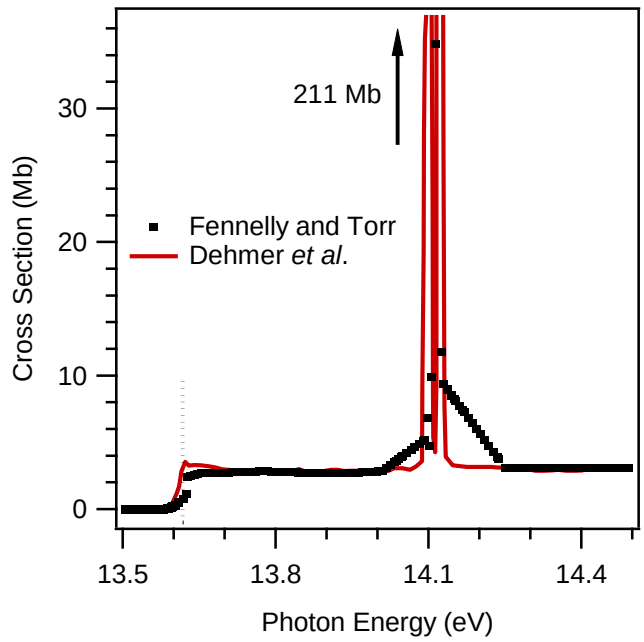

FIG. S2. Absolute photoionization spectrum of O(^3P) from literature. The absolute photoionization spectrum (black dots) was reported by Fennelly and Torr,[8] which is an evaluation of the absolute cross section measurements reported by Samson and co-workers[6,9] and the high-resolution relative spectrum published by Dehmer *et al*.[7] The red line in this figure is the new digitization of the Dehmer *et al*. spectrum, scaled to the absolute value reported at 14.25 eV by Angel and Samson .

III. DETECTION OF OH(v>0) IN THE O(^1D) + H_2 SYSTEM

In the main text, we observed the formation of OH radicals at their parent mass (m/z = 17) from the reaction of O(^1D) atoms with H_2O. In this section, we demonstrate the appearance of OH(v>0) in the O(^1D) + H_2 reaction system.

We conducted preliminary experiments to detect OH formed from reactions of O(^1D) with H_2. In this chemical system, a significant number of H atoms were formed, which subsequently reacted with the ozone precursor to form highly vibrationally-excited OH radicals (with excitations up to v=9)[10]. As seen in the O(^1D) + H_2O chemistry described in the text, we observed large signals at early times at m/z = 17 in this chemical system, presumably from OH(v>0), followed by the slower decay similar to that expected for OH(v=0). At photon energies below the ionization energy of ground state OH, the long-lived OH signal disappeared, yet we still observed the fast component. Figure S3 shows the fast m/z = 17 decay for experiments conducted at 12.588 eV, which was below the ionization energy of OH. Similar experiments, carried out with the photon energy set to 13.103 eV (shown in Fig. S3, red trace) showed the time-dependent behavior of the OH radicals in the O(^1D) + H_2 reaction system when they were detected above the ionization energy. Both traces rose nearly instantaneously with the same formation rate, but whereas the OH signal measured at 12.588 eV decayed almost immediately (disappearing completely by 2 ms), the signal measured at 13.103 eV had a lifetime similar to that expected for a species that is primarily being removed by a slow bimolecular reaction. We hypothesize that the ions detected at m/z = 17 at 12.588 eV are OH radicals formed with some degree of vibrational excitation, appearing as hot bands below the adiabatic ionization energy of ground state OH radicals. The vibrational excitation of these OH radicals was rapidly quenched by the high concentrations of H_2O and O_2 in the reaction system,[11,12] converting OH(v>0) into OH(v=0), which could not be ionized by 12.588 eV

photons. The signal observed at 13.103 eV had contributions from both OH(v>0) and OH(v=0), with the rapidly decaying, early part of the kinetics trace coming from ionization of OH(v>0) and the slower component from OH(v=0). The same process would likely occur in the O(^1D) + H_2O system, described in the main text of the paper, although to a lesser extent because this reaction system yields fewer H atoms and subsequently fewer vibrationally-excited OH radicals.

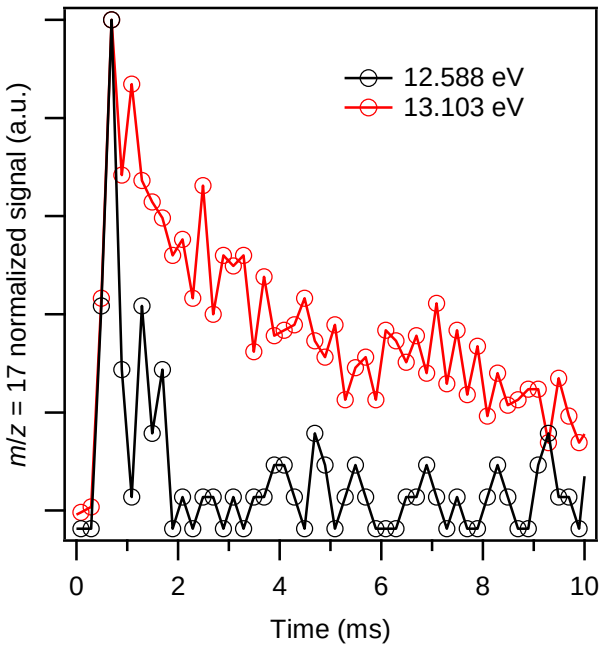

FIG. S3. Observed m/z = 17 signal below (12.588 eV, black trace) and above (13.103 eV, red trace) the ionization energy of OH(v=0).

IV. COMPUTED PHOTOIONIZATION SPECTRUM OF OH

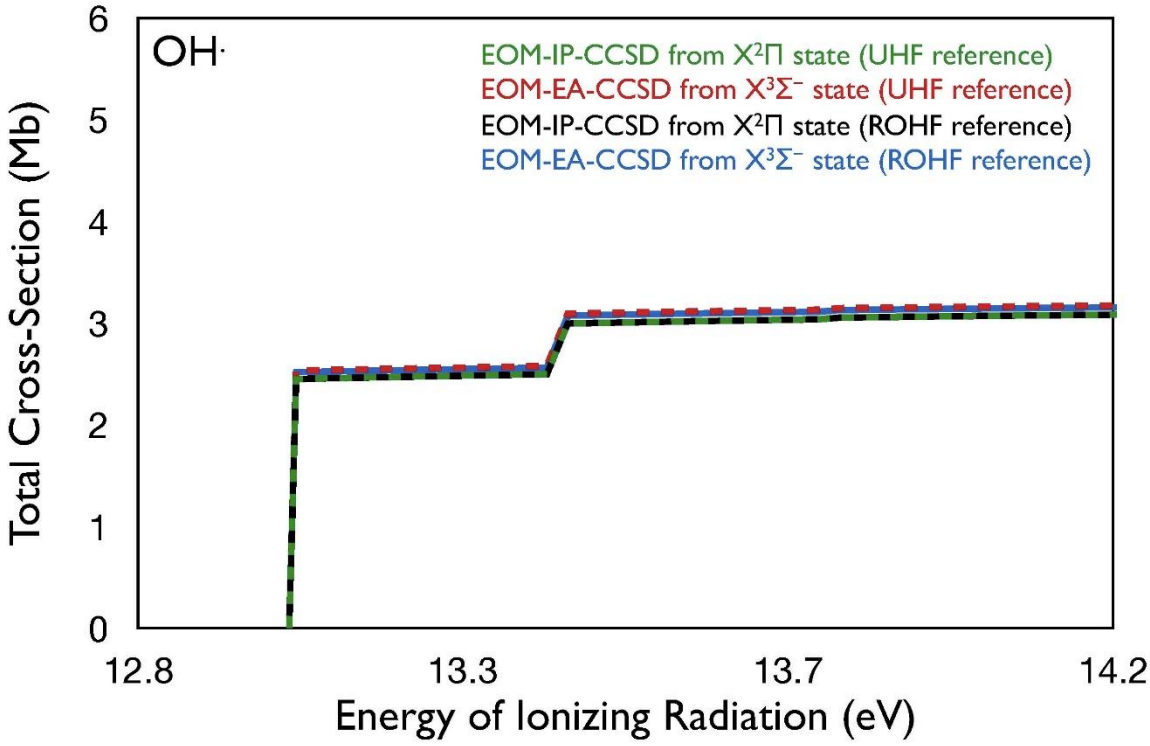

FIG. S4. Absolute photoionization cross sections for OH radical computed using EOM-IP-CCSD (from the doublet $X\ ^2\Pi$ state) and EOM-EA-CCSD (from the triplet $X\ ^3\Sigma^-$ state). Results are shown for both UHF and ROHF reference wave functions.

V. COMPUTED PHOTOIONIZATION SPECTRUM OF O

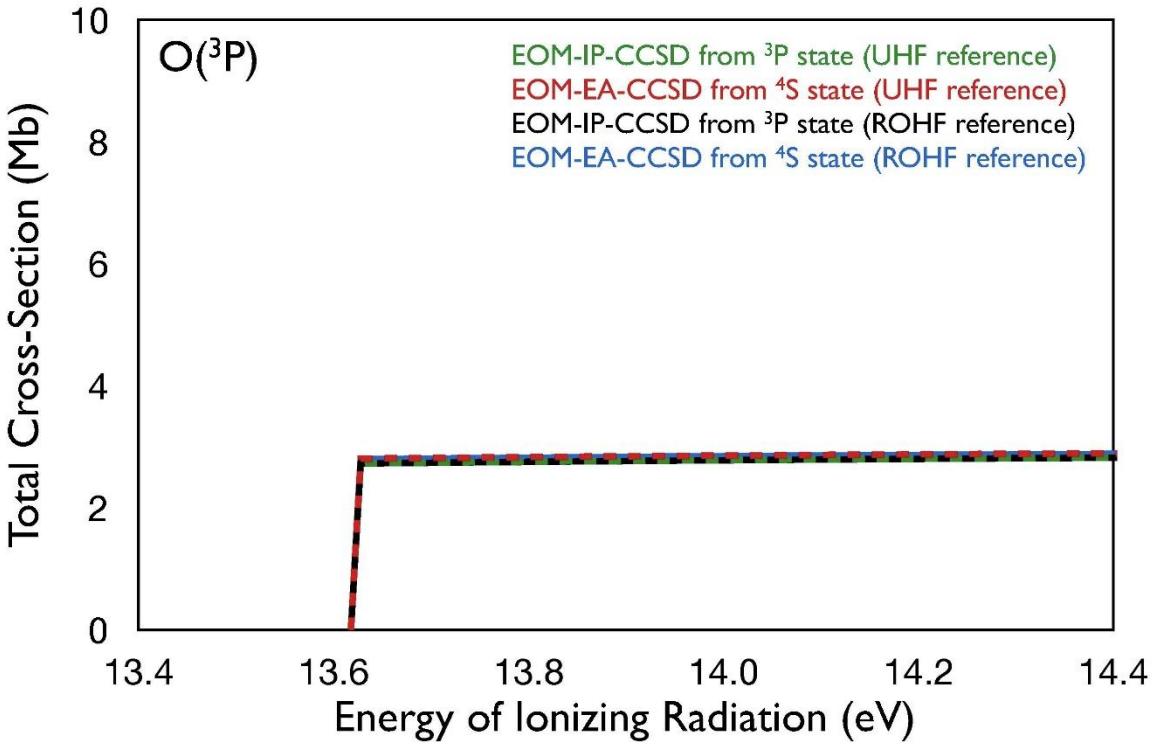

FIG. S5. Absolute photoionization cross sections for O(^3P) computed using EOM-IP-CCSD (from the triplet ^3P state) and EOM-EA-CCSD (from the quartet ^4S state). Results are shown for both UHF and ROHF reference wave functions.

VI. OH CROSS SECTIONS AND UNCERTAINTIES

For each experiment *i* listed in Table I of the main text, we independently determined the photoionization cross section of OH ($\sigma_{\mathrm{OH}}(E), i$) and the relative uncertainty at the corresponding photon energy, listed in Table S1. The average OH photoionization cross section for each photon energy was then computed from the weighted mean of all *p* measurements performed at that energy (*p* = 5 at 14.193 eV and *p* = 9 at 13.436 eV). The relative standard errors (RSE) for the reported cross sections, $RSE\left(\sigma_{\mathrm{OH}}(E), \mathrm{total}\right)$, were computed using equation (S1).

(S1) $$RSE\left(\sigma_{\mathrm{OH}}(E), \mathrm{total}\right) = \sqrt{\frac{p}{\sum_{i=1}^{p}\left(1/\,RSE_i^2\left(\sigma_{\mathrm{OH}}(E)\right)\right)}}$$

There were a number of sources of uncertainty, both systematic and random. These included ion counting statistics, modeling of the photolysis yields and radical concentrations, precursor flows and concentrations, and literature values of reference photoionization cross sections. The systematic errors were summed in quadrature along with the random errors, because there were a large number of uncorrelated systematic errors. In the following sections, we describe the evaluation and error analysis of the cross sections at the two energies.

A. Uncertainty in $\sigma_{\mathrm{OH}}(14.193\ \mathrm{eV}), i$

1. Expression for relative standard error

At 14.193 eV, we determined the cross section σ_{OH} relative to $\sigma_{O(3P)}$ by directly measuring the OH and O(^3P) signals and calculating (from the kinetics model) the concentrations in the same experiment. The uncertainty in the cross section measurement for each experiment conducted at 14.193 eV was calculated from:

(S2)

$$RSE_i\left(\sigma_{OH}(14.193\text{ eV})\right) = \left(RSE^2\left(N_{OH,max}/N_{O(3P),max}\right) + RSE^2\left(S_{OH}/N_{OH}\right) + RSE^2\left(\sigma_{O(3P)}(14.193\text{ eV})\right)\right)^{1/2}$$

where the contributions to the relative uncertainty in the OH cross section were:

$RSE\left(N_{OH,max}/N_{O(3P),max}\right)$: systematic uncertainty in the ratio of the modeled peak OH concentration to the modeled peak O(^3P) concentration resulting from *uncertainties in the rate constants in the kinetics model*, *uncertainty in the O(^1D) yield from ozone photolysis* $\Phi_{O3,248}\left(^1D\right)$, and *uncertainty in the ozone concentration*, N_{O3}. See below (Analysis of systematic errors). Typical values: 23–47%.

$RSE\left(S_{OH}/N_{OH}\right)$: random error from fitting the measured OH signal (S_{OH}) to the modeled OH kinetics trace (N_{OH}). This term included statistical noise in the ion signal and any deviation of the model and the observed time profiles. Typical values: 4%.

$RSE\left(\sigma_{O(3P)}\left(14.25\text{ eV}\right)\right)$: uncertainty in the literature cross section of O(^3P) at 14.25 eV. Value equal to 10%.[6]

2. Analysis of systematic errors

In determining the first term in equation (S2), we evaluated the systematic errors in modeling OH and O(^3P) concentrations. These came from: (a) uncertainties in the rate constants used in the kinetics model (Table 2), (b) uncertainty in the photodissociation quantum yield of O(^1D) ($\Phi_{O3,248}\left(^1D\right)$), and (c) uncertainty in the initial ozone concentration, N_{O3}. We determined the RSE for N_{OH} and $N_{O(3P)}$ and the ratio $N_{OH}/N_{O(3P)}$ by performing Monte Carlo simulations (1000 iterations) for each of these three uncertainties.

The variances in N_{OH} and $N_{O(3P)}$ were often correlated. For example, the dependence of the uncertainties in modeled peak O(^3P) and peak OH concentrations on initial N_{O3} were positively correlated and largely canceled upon taking the ratio of the time-dependent concentrations. We therefore found it necessary to compute uncertainty in the ratio of $N_{OH}/N_{O(3P)}$ and not just the individual uncertainties in the concentrations when determining $RSE\left(N_{\mathrm{OH,max}} / N_{\mathrm{O}(3P),\mathrm{max}}\right)$.

a. Uncertainty in the rate constants in the kinetics model:

In our simulation varying the rate constants, we found that the contribution to $RSE\left(N_{\mathrm{OH,max}} / N_{\mathrm{O}(3P),\mathrm{max}}\right)$ was 5.0–11.5 %. We evaluated this error for each set of experimental conditions and include an uncertainty term in our analysis reflecting this error, which is roughly equal to the sum of the uncertainty in both concentrations.

We found that the modeled peak OH concentration was negatively correlated with the modeled peak O(^3P) concentration, i.e. that the relative standard error in the ratio varying only the set of rate constants $\{k\}$ was approximately

(S3) $$RSE\left(N_{\mathrm{OH,max}} / N_{\mathrm{O}(3P),\mathrm{max}};\{k\}\right) \approx RSE\left(N_{\mathrm{OH,max}};\{k\}\right) + RSE\left(N_{\mathrm{O}(3P),\mathrm{max}};\{k\}\right)$$

Had they been uncorrelated, these would have been added in quadrature leading to a smaller final RSE.

In general, the term that dominated the overall reaction mechanism in this system was the reaction between two OH radicals. This rate has been evaluated with an uncertainty of 25%.[13] Increasing the rate of the OH self-reaction resulted in a decrease in the peak OH concentration, while increasing the amount of O(^3P) formed from this reaction. Therefore, peak OH decreased as

peak O(^3P) increased, leading to an overall increase in the uncertainty of peak OH divided by peak O(^3P).

b. Uncertainty in the quantum yield of O(^1D) from ozone photodissociation at 248 nm $\Phi_{\mathrm{O3,248}}\left(^1D\right)$*:*

In our Monte Carlo simulation with $\Phi_{\mathrm{O3,248}}\left(^1D\right) = 0.90 \pm 0.09$ [13-15] we found that $RSE\left(N_{\mathrm{OH,max}} / N_{\mathrm{O}(3P),\mathrm{max}}; \left\{\Phi\left(^1D\right)\right\}\right)$ among the 5 experiments was in the range 20–47 %. This was the largest contribution to the uncertainty in $N_{\mathrm{OH,max}} / N_{\mathrm{O}(3P),\mathrm{max}}$. We again found that the modeled peak OH concentration was negatively correlated with the modeled peak O(^3P) concentration when varying $\Phi_{\mathrm{O3,248}}\left(^1D\right)$. We evaluated this error for each experiment and included an uncertainty in the ratio of modeled peak OH and modeled peak O(^3P); these were close to the sum of the uncertainties in the modeled concentrations.

Increasing $\Phi_{\mathrm{O3,248}}\left(^1D\right)$ led to more initial OH generated from reaction of O(^1D) + H_2O, while simultaneously decreasing the amount of O(^3P) formed from direct photodissociation. While some of the formed O(^1D) was quenched to O(^3P), the peak O(^3P) was still reduced.

c. Uncertainty in the initial ozone concentration:

We evaluated the effect of changing the initial ozone concentration by ±4.5% (the systematic uncertainty in N_{O3}) on the peak OH and O(^3P) concentrations. These values were positively correlated, as increasing O_3 increased both the initial O(^1D) radical concentration (thereby increasing the initial OH concentration) and the initial O(^3P) concentration. Taking the

ratio of peak OH with peak O(^3P) resulted in negligible uncertainty (<0.3%) in the OH cross section measurement at 14.193 eV.

B. Cross section $\sigma_{\mathrm{OH}}(13.436\ \mathrm{eV})$ and its uncertainty

1. Determination of σ_{OH} at 13.436 eV

At 13.436 eV, we measured the OH cross section relative to that of xenon using equation IV from the text.

(S4) $$\sigma_{\mathrm{OH}}(E) = \sigma_{\mathrm{Xe}}(E) \times \frac{\alpha_{\mathrm{Xe}} \times f_{\mathrm{Xe},132}}{\alpha_{\mathrm{OH}} \times f_{\mathrm{OH},17}} \times \frac{\left\langle \frac{S_{\mathrm{OH}}(E,t)}{N_{\mathrm{OH}}(t)} \right\rangle_{\Delta t}}{\left\langle \frac{S_{\mathrm{Xe}}(E,t)}{N_{\mathrm{Xe}}(t)} \right\rangle_{\Delta t'}}$$

Concentrations of most stable precursor and buffer gases in the reactor were calculated from flow and pressure conditions. However, the xenon concentration could not be determined accurately, because the xenon gas flow rates used in these experiments (0.5 sccm) were at the lower limit of the flow controller range. The systematic uncertainty in this range specified by the manufacturer was ±40%, but we expected that the precision and reproducibility were substantially better. The actual xenon concentration N_{Xe} was then related to the xenon concentration estimated from the flow conditions $N_{\mathrm{Xe,flow}}$ by a scale factor, c_{Xe},

(S5) $$N_{\mathrm{Xe}} = c_{\mathrm{Xe}} \times N_{\mathrm{Xe,flow}}$$

To determine the c_{Xe}, we used the data from the 14.193 eV experiments where both Xe and O(^3P) were ionized. We calculated N_{Xe} relative to the O(^3P) concentration in the cell by measuring the Xe^+ and O^+ ion signals using the known photoionization cross sections.[6,16] We then obtained

the scaling factor, c_{Xe} from the ratio of the experimentally determined $\left\langle N_{\mathrm{Xe}}(t)\right\rangle_{\Delta t}$ to the Xe concentration estimated from the gas flow rates $N_{\mathrm{Xe,flow}}$.

(S6) $$c_{\mathrm{Xe}} = \frac{\left\langle N_{\mathrm{Xe}}(t)\right\rangle_{\Delta t}}{N_{\mathrm{Xe,flow}}} = \frac{1}{N_{\mathrm{Xe,flow}}} \times \frac{\sigma_{\mathrm{O}(3P)}(E)}{\sigma_{\mathrm{Xe}}(E)} \times \frac{\alpha_{\mathrm{O}(3P)} \times f_{\mathrm{O}(3P),16}}{\alpha_{\mathrm{Xe}} \times f_{\mathrm{Xe},132}} \times \frac{\left\langle S_{\mathrm{Xe}}(E,t)\right\rangle_{\Delta t}}{\left\langle \frac{S_{\mathrm{O}(3P)}(E,t)}{N_{\mathrm{O}(3P)}(t)} \right\rangle_{\Delta t'}}$$

By averaging over all experiments performed at 14.193 eV, we obtained a scaling factor of $\overline{c_{\mathrm{Xe}}}$ = 0.89±0.04, where the error bars are only the statistical uncertainty, i.e. the standard deviation of the mean (and exclude any systematic uncertainties). The reproducibility in c_{Xe} was much better than the ±40% systematic uncertainty in the measured flow of Xe from the mass flow controller readings.

The cross section at 13.436 eV was then given by:

(S7) $$\sigma_{\mathrm{OH}}(E) = \sigma_{\mathrm{Xe}}(E) \times \frac{\alpha_{\mathrm{Xe}} \times f_{\mathrm{Xe},132}}{\alpha_{\mathrm{OH}} \times f_{\mathrm{OH},17}} \times \frac{\left\langle \frac{S_{\mathrm{OH}}(E,t)}{N_{\mathrm{OH}}(t)} \right\rangle_{\Delta t}}{\left\langle \frac{S_{\mathrm{Xe}}(E,t)}{\overline{c_{\mathrm{Xe}}} \times N_{\mathrm{Xe,flow}}} \right\rangle_{\Delta t'}}$$

This expression was used to compute σ_{OH} at 13.436 eV for each of the nine experiments.

In effect, the cross section at 13.436 eV was determined relative to the average of the O(^3P) cross section measured at 14.193 eV. The net result of these two equations (S6) and (S7) was that σ_{OH} for each of the nine experiments at 13.436 eV was given by:

(S8) $$\sigma_{\mathrm{OH}}(13.436) \propto \sigma_{\mathrm{O}(3P)}(14.193) \times \left\langle \frac{S_{\mathrm{OH}}(13.436,t)}{N_{\mathrm{OH}}(13.436,t)} \right\rangle_{\Delta t} \Bigg/ \overline{\left\langle \frac{S_{\mathrm{O}(3P)}(14.193,t)}{N_{\mathrm{O}(3P)}(14.193,t)} \right\rangle_{\Delta t'}}$$

where the overbar indicates the weighted averaging over all five experiments done at 14.193 eV.

2. Uncertainty in the cross section at 13.436 eV

The determination of the uncertainties in σ_{OH} at 13.436 eV differed from the analysis at 14.193 eV, because S_{OH} and $S_{O(3P)}$ were measured in different experiments using xenon as a transfer standard. The uncertainty in the cross section measurement for each experiment conducted at 13.436 eV was calculated from:

(S9)

$$RSE_i\left(\sigma_{OH}(13.436\text{ eV})\right) = \left(RSE^2\left(N_{OH,max}\left(13.436\right) / \overline{N_{O(3P),max}\left(14.193\right)}\right) + RSE^2\left(S_{OH} / N_{OH}\right) + RSE^2\left(\sigma_{O(3P)}(14.193\text{ eV})\right) + RSE^2\left(\sigma_{Xe}\left(13.436\text{ eV}\right)\right) + RSE^2\left(c_{Xe}\right)\right)^{1/2}$$

The second and third terms on the right hand side of equation (S9) are the same as those that appear in equation (S2). The other terms are the contributions to the relative uncertainty in the OH cross section from:

$RSE\left(N_{OH,max}\left(13.436\right) / \overline{N_{O(3P),max}\left(14.193\right)}\right)$: systematic uncertainty in the ratio of the modeled peak N_{OH} in a given 13.436 eV experiment to the average modeled peak $N_{O(3P)}$ in all 14.193 eV experiments due to *uncertainties in the rate constants in the kinetics model*, *uncertainty in the O(^1D) yield from ozone photolysis* $\Phi_{O3,248}\left(^1D\right)$, and *uncertainty in the ozone concentration*, N_{O3}. We analyzed the effect of these systematic parameters in a manner similar to section IV.A.2. Although the numerator and denominator were determined in different experiments (and the denominator was a weighted average of five experiments), we found in Monte Carlo simulations that there were significant correlations in N_{OH} and $N_{O(3P)}$ when varying each of these parameters ($\{k\}$, $\Phi_{O3,248}\left(^1D\right)$, N_{O3}). The RSE values for the concentrations added almost linearly rather than

in quadrature. The correlations likely persisted because the experimental conditions in the two sets of experiments were similar, and hence the modeled peak concentrations at 13.436 eV behaved similarly those at 14.193 eV. The dominant term was again due to the uncertainty in $\Phi_{O3,248}\left(^1D\right)$. Typical values: 26–29%.

$RSE\left(\sigma_{Xe}(13.436\text{ eV})\right)$: uncertainty in the literature cross section of Xe at 13.436 eV. Value equal to 2%.[16]

$RSE\left(c_{Xe}\right)$: random error in the measurement of the Xe scaling factor from experiments at 14.193 eV. Value equal to 4%.

TABLE S1. Evaluated OH photoionization cross sections (Mb) and percent relative uncertainties for each experiment at a given energy (eV).

Experiment #	Photon Energy (eV)	Evaluated OH Cross Section (Mb)	Cross Section Uncertainty
2	13.436	2.8	29%
3	13.436	3.7	30%
4	13.436	3.7	30%
5	13.436	4.0	30%
6	13.436	3.3	29%
7	13.436	2.6	29%
8	13.436	4.3	30%
9	13.436	4.6	30%
10	14.193	5.1	45%
11	14.193	6.2	26%
12	14.193	6.2	29%
13	14.193	3.9	28%
14	13.436	2.6	29%
15	14.193	3.6	48%

VII. ABSOLUTE PHOTOIONIZATION SPECTRUM OF OH

The absolute photoionization spectrum of OH is reported as tabulated data in Table S2. The variance of the cross sections obtained by scaling the relative photoionization spectrum to the two absolute single-energy cross section values is equal to the average of the two single-energy variances.

TABLE S2. Absolute photoionization spectrum of OH. A relative spectrum was scaled to absolute measurements as outlined in the text. The relative error of the absolute cross sections reported is $RSE(\sigma_{OH}(E)) = 32\%$.

Photon energy (eV)	**OH (Mb)**	**Photon energy (eV)**	**OH (Mb)**
12.513	0.026	**13.413**	2.805
12.563	0.140	**13.463**	3.219
12.613	0.061	**13.513**	5.362
12.663	−0.007	**13.563**	11.004
12.713	−0.108	**13.613**	6.315
12.763	0.115	**13.663**	5.612
12.813	0.047	**13.713**	3.916
12.863	−0.128	**13.763**	3.526
12.913	0.265	**13.813**	4.396
12.963	0.656	**13.863**	3.859
13.013	2.558	**13.913**	4.068
13.063	2.777	**13.963**	3.908
13.113	3.139	**14.013**	3.765
13.163	2.512	**14.063**	3.129
13.213	2.522	**14.113**	2.112
13.263	2.948	**14.163**	2.769
13.313	2.592	**14.213**	5.354
13.363	2.550		

REFERENCES

[1]J. Berkowitz, Int. J. Mass Spectrom. **271**, 8 (2008).
[2]G. R. Cook, Trans. Am. Geophys. Union **49**, 736A (1968).
[3]G. R. Cook, in *Recent Developments in Mass Spectroscopy*, edited by K. Ogata, and T. Hayakawa (University Park Press, Japan, 1970), pp. 761.
[4]A. Mocellin, K. Wiesner, F. Burmeister, O. Björneholm, and A. Naves de Brito, J. Chem. Phys. **115**, 5041 (2001).
[5]M. J. Weiss, J. Berkowitz, and E. H. Appelman, J. Chem. Phys. **66**, 2049 (1977).
[6]G. C. Angel, and J. A. R. Samson, Phys. Rev. A **38**, 5578 (1988).
[7]P. M. Dehmer, J. Berkowitz, and W. A. Chupka, J. Chem. Phys. **59**, 5777 (1973).
[8]J. A. Fennelly, and D. G. Torr, At. Data Nucl. Data Tables **51**, 321 (1992).
[9]J. A. R. Samson, and P. N. Pareek, Phys. Rev. A **31**, 1470 (1985).
[10]W. B. DeMore, J. Chem. Phys. **47**, 2777 (1967).
[11]D. C. McCabe, B. Rajakumar, P. Marshall, I. W. M. Smith, and A. R. Ravishankara, Phys. Chem. Chem. Phys. **8**, 4563 (2006).
[12]L. D'Ottone, D. Bauer, P. Campuzano-Jost, M. Fardy, and A. J. Hynes, Phys. Chem. Chem. Phys. **6**, 4276 (2004).
[13]S. P. Sander, J. Abbatt, J. R. Barker et al., JPL Publication 10-6 2011).
[14]Y. Matsumi, and M. Kawasaki, Chem. Rev. **103**, 4767 (2003).
[15]R. Atkinson, D. L. Baulch, R. A. Cox, J. N. Crowley, R. F. Hampson, R. G. Hynes, M. E. Jenkin, M. J. Rossi, and J. Troe, Atmos. Chem. Phys. **4**, 1461 (2004).
[16]J. A. R. Samson, and W. C. Stolte, J. Electron Spectrosc. Relat. Phenom. **123**, 265 (2002).